frontiers | Frontiers in Earth Science

TYPE Original Research
PUBLISHED 12 December 2024
DOI 10.3389/feart.2024.1486831

OPEN ACCESS

EDITED BY
Yifei Sun,
Taiyuan University of Technology, China

REVIEWED BY
Xiangfeng Guo,
South China University of Technology, China
Xiaodong Ni,
Hohai University, China
Li Cheng,
University of Western Australia, Australia
Congyang Yu,
University of Western Australia, Australia, in collaboration with reviewer LC

*CORRESPONDENCE
Leiming Zheng,
zlm0327@hhu.edu.cn

RECEIVED 20 September 2024
ACCEPTED 25 November 2024
PUBLISHED 12 December 2024

CITATION
Zhao Z and Zheng L (2024) Influences of the geogrid-reinforced soil platform on the performance of pile-supported embankment. *Front. Earth Sci.* 12:1486831. doi: 10.3389/feart.2024.1486831

Influences of the geogrid-reinforced soil platform on the performance of pile-supported embankment

Zhihui Zhao[1] and Leiming Zheng[2]*

[1]Suzhou New District Testing Corporation, Suzhou, China, [2]College of Harbour, Coastal and Offshore Engineering, Hohai University, Nanjing, China

Geosynthetic-reinforced pile-supported embankments have seen widespread adoption worldwide in recent years due to their cost-effectiveness and construction efficiency. In this system, the conventional pile cap is replaced by the geogrid-reinforced soil platform (GRSP), which enhances horizontal load transfer to stabilize the embankment. This study investigates the influences of GRSP on the behavior of pile-supported embankments through field testing and numerical computation. The measured results of field testing indicate that a well-compacted GRSP reduces the lateral displacement of the embankment and changes the development of pressures acting on pile and soil. Numerical analysis demonstrates that both soil arching and tensioned membrane effects effectively transfer loads from the soil to the piles, with the tensioned membrane effect typically being more prominent. The characteristics of the GRSP have a significant impact on both effects, with elastic modulus, tensile stiffness, and friction angle being the three most crucial parameters for reducing embankment settlement.

KEYWORDS

pile-supported embankment, reinforced soil platform, geogrid, load transfer, field test, numerical analysis

1 Introduction

A large number of highway embankments are constructed on soft soil, and the geosynthetic-reinforced pile-supported embankments have been increasingly adopted all over the world in the recent years (Liu et al., 2007; 2015; Xing et al., 2014; Esmaeili et al., 2018; Wu et al., 2022; Du et al., 2024) owing to their high cost effectiveness and construction efficiency. In this system, piles (i.e., concrete pile, deep mix column, and stone pile) reinforce the soft soil vertically and are important to impart the loads from the embankment to deeper firm soil (Pham et al., 2004; Stewart et al., 2004; Huang et al., 2009). The geosynthetic-reinforced soil platform (GRSP) enhances horizontal load transfer to stabilize the embankment, and the conventional pile cap is replaced by GRSP, allowing the load between piles to be partially transferred to the pile head (Han J. and Gabr M. A., 2002; Briançon and Simon, 2012; Rowe and Liu, 2015). The GRSP consists of a single or multiple geosynthetic layers (such as geogrid) and soil, with the cohesionless soil being commonly used in practice due to drainage and consolidation of foundation soil under embankment loading. Since the piles bear the majority of the embankment load, the stress on the foundation soil is substantially reduced, leading to a decrease in both vertical and lateral

displacements of the embankment. Consequently, this approach allows for the construction of higher embankments on soft soil. The behavior of geosynthetic-reinforced pile-supported embankment was investigated by model experiments (Blanc et al., 2013; Okyay et al., 2014; Rui et al., 2019; Shen et al., 2020), full-scale field tests (Briançon and Simon, 2012; Zhou et al., 2016; van Eekelen et al., 2020; Terqueux et al., 2023), and numerical simulations (Huang and Han, 2010; Borges and Marques, 2011; Rowe and Liu, 2015; Badakhshan et al., 2020; Ghosh et al., 2021; Khosrojerdi et al., 2018). The performance of load transfer from soft soil to piles has been widely acknowledged as the soil arching effect in embankments (Terzaghi, 1943). Apart from the model proposed by Terzaghi (1936), various methods have been introduced to model the soil arching effect (Xu et al., 2018; Yan et al., 2022; Zhang et al., 2022). However, these models generally ignored the influence of the GRSP and the supporting effect of the foundation soil between piles. In addition to the soil arching effect, the tensioned membrane or stiffened platform effect of the GRSP and the stiffness difference between the pile and soil in foundation are load transfer mechanisms (Han J. and Gabr M. A., 2002). Based on the load transfer mechanisms revealed by field or laboratory testing, many design methods have been proposed, but some of them yield quite different results, especially in the tension force of geosynthetics in the GRSP and the stress reduction ratio (Stewart and Filz, 2005; Chen et al., 2010; Rowe and Liu, 2015).

Several studies have addressed the GRSP, primarily focusing on the role of geosynthetics within the system. Analyses have examined how the stiffness of geosynthetics affects the performance of pile-supported embankments, revealing that geosynthetic properties within the GRSP can significantly influence embankment behavior (e.g., settlement and soil arching) and foundation performance (e.g., load transfer efficiency from the soil to pile and differential settlement between the pile and soil) (Han and Gabr, 2002; Huang and Han, 2010).The distribution of tensile force and strain of geosynthetics was obtained via numerical computation and field testing, revealing that the maximum strain and tensile force occur at the edge of pile heads after the completion of the embankment construction (Han J. and Gabr M. A., 2002; Liu et al., 2007; Huang et al., 2009). Furthermore, the effects of multiple layers of geosynthetic reinforcement on the performance of the pile-supported embankment were discussed via field testing and numerical analysis (Briançon and Simon, 2012; Rowe and Liu, 2015). In addition to the effect of geosynthetics in GRSP, the soil in GRSP also influences the load mechanism. As a result of the penetration of the pile head into the GRSP soil (i.e., gravel), the GRSP soil partially moves to the soil surface surrounding the pile, ensuring that the upper loads act on the foundation soil continuously. The contact surface force between geosynthetics and soil in GRSP is influenced by the tensile force in geosynthetics. In summary, the characteristics of the GRSP have significant influences on the load transfer mechanism of the embankment and foundation.

The objective of this study is to report the influences of GRSP on the performance of the pile-supported embankment, and the effect of the compaction of GRSP materials is studied by comparative field testing. Moreover, based on field testing, parametric studies of GRSP materials, including both soil and geogrid, are conducted via the finite-element analysis. The performances of the pile-supported embankment investigated using the numerical analysis include the stress concentration ratio of pile to soil, soil arching effect, tensioned membrane effect, differential settlement of pile and soil, settlement of the embankment surface, and height of the plane of equal settlement in the embankment and its settlement.

TABLE 1 Soil properties.

Soil layer	Thickness/m	Status	Shear resistance/kPa
Loam	2.0	Plastic	17.4
Muddy clay	8.4	Fluidal plastic	16.5
Sandy loam	3.2	Soft plastic	23.3
Sandy clay	7.4	Plastic	31.4
Silty sand	10.8	Medium dense	39.2

2 Full-scale field test

2.1 Site conditions

The site is located in a suburb of Jiangsu province, China. The soil profile is as follows: there is a 2.0-m-thick loam overlying an 8.4-m-thick deposit of fluidal plastic muddy clay; this deposit overlies soft, plastic, sandy loam of approximately 3.2 m thick. A sandy clay layer of approximately 7.4 m thick lies beneath the soft sandy loam, followed by a deeper layer of medium-density silty sand of approximately 10.8 m thick. The ground water level was 1.2 m high. The soil properties are listed in Table 1.

2.2 Geogrid-reinforced pile-supported highway embankment

The highway embankment is 5.7 m high and 249 m long with a crown width of 35 m. The side slope is 1V: 1.5H. The filling material mainly consists of pulverized fuel ash and clay with the cohesion of 10 kPa, the angle of friction of 26°, and the average unit weight of 18.5 kN/m^3. The cross-sectional view of the testing embankment and the locations of instruments are illustrated in Figure 1.

The embankment is supported by Cast-*in situ* concrete large-diameter pipe (PCC) pile (Liu et al., 2007). The minimum compressive strength of the concrete is 15 MPa. The pipe piles are 16 m in length, the outer diameter of each pile is 1.0 m, and the thickness of the concrete annulus is 120 mm. The pipe piles are arranged in a square pattern at a spacing of approximately three times the pile diameter (3.3 m) from the center to the center of the adjacent piles. The replacement ratio, defined as the percent coverage of the pile annular area over the total foundation area, is 3.1%. A 0.5-m-thick gravel layer is placed on the top of piles, in which two layers of a biaxial polypropylene geogrid are sandwiched. One layer of the geogrid is placed in the middle of the gravel layer, and the other is placed on the top of the gravel layer. The gravel and geogrid form the composite-reinforced bearing

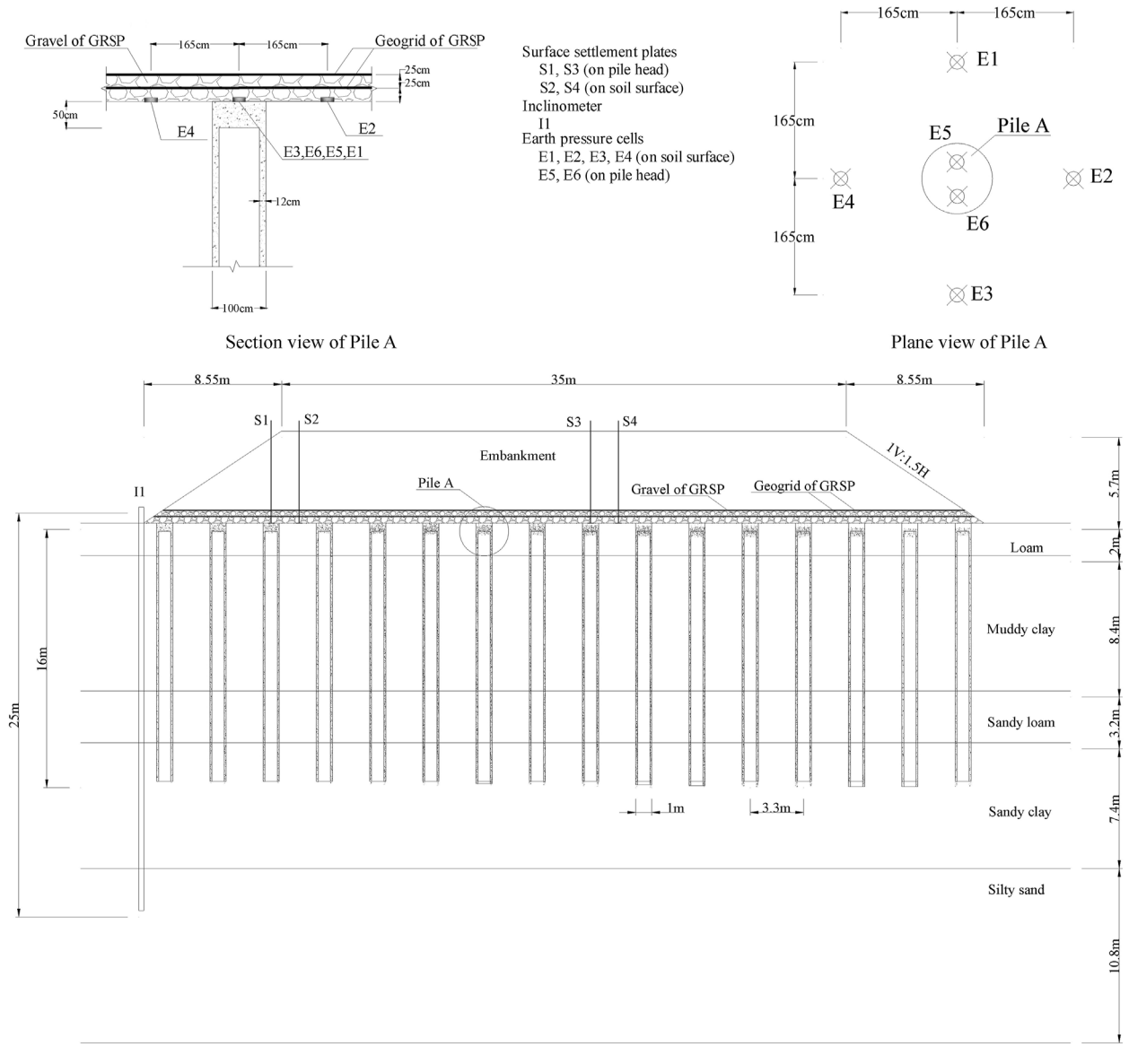

FIGURE 1
Cross-section of the instrumented embankment.

layer between the embankment and pile-reinforced foundation, and the composite-reinforced bearing layer is named GRSP, which is shown in Figure 1. The tensile strength in the longitudinal and latitudinal directions of the geogrid is 90 kN/m, and the natural dry density and the maximum dry density of platform gravel are 1.43 kN/m^3 and 1.87 kN/m^3, respectively. The details of the geogrid-reinforced platform construction are as follows:

First,, a 0.25-m layer of gravel is placed on top of the piles for platform construction, followed by compaction. Next, the first layer of the geogrid is installed. A second 0.25-m layer of gravel is then placed using two different methods for placement: i) spreading and compacting the gravel from the platform center toward both sides using a 4-ton vibratory compactor to achieve a compaction degree of over 90% and ii) placing the gravel from one side to the other without compaction. Finally, the second geogrid layer is installed atop the gravel. These two construction methods for the geogrid-reinforced platform lead to different gravel densities and interaction forces between the geogrid and gravel before embankment filling. The first method (with compaction) produces a higher gravel strength and greater contact force between the geogrid and gravel than the second method (without compaction). For both construction methods, the geogrid was wrapped and anchored back into the platform or embankment over 5 m long at the edges of the embankment.

In order to monitor the performance of the embankment during construction, various instruments were installed *in situ* (Figure 1). The installed instruments are detailed as follows: i) earth pressure cells were used to measure the vertical loads shared by piles and the surrounding soil. Cells measuring load directly on the pile were installed at the pile heads, with a measuring range of 0–1.0 MPa. Additional cells measuring the load carried by the soils were fixed on the surface of

the surrounding soil beneath the GRSP (Figure 1) and measured using portable readout equipment. ii) Four settlement plates were installed at the pile head level, both near the shoulder of the embankment and in the center. One was on the top of the pile, and the other was in the surrounding soil in the middle of the pile spacing. The vertical settlements were monitored using digital level gauges. iii) A vertical inclinometer, 25 m in length, was installed at the embankment toe. All the instruments were installed after the completion of pile construction but before building GRSP and embankment. The field monitoring started with the construction of GRSP and lasted approximately 5 months after the completion of the embankment.

3 Numerical model calibration and parametric study

In order to investigate the influences of GRSP parameters on the performance of the pile-supported embankment, a 2D axisymmetric model was used to simulate the single pile and the surrounding soil with the finite element software PLAXIS. The constitutive models, simulation of construction, and modeling procedures are described below.

The embankment fill, gravel of GRSP, and foundation soils are modeled as linearly elastic, perfectly plastic materials obeying the Mohr–Coulomb failure criteria. The Mohr–Coulomb model requires five parameters: effective cohesion, inner friction angle, dilatancy angle, effective Young's modulus, and Poisson's ratio, as outlined in Table 2. These parameters were derived from the geotechnical investigation report for Yancheng, Jiangsu Province, with the dilatancy angle assumed to be 0°. The pile is modeled as an isotropic linear elastic material with a Young's modulus of 20 GPa and a Poisson's ratio of 0.2. The geogrid in GRSP is modeled as a geogrid element incorporated into the software, which can sustain axial tensile force only, and the tensile stiffness of geogrid is 1,125 kN/m. Furthermore, the interface yield stress is also determined by the Mohr–Coulomb failure criteria, and a reduction factor of 0.7 is applied to the pile–soil contact face and geogrid–gravel contact face, based on the shear strength of GRSP gravel and foundation soil.

The modeling procedure consists of two main steps: to construct initial soil stress field and to model six-staged embankment construction. The staged embankment construction includes six filling steps to the top of the embankment in simulation.

The parametric study on the characteristics of the GRSP was carried out, and the baseline case is the field testing mentioned above. The values of all influencing factors are listed in Table 3. In addition, one parameter was deviated from the baseline case at one time to explore the influences of the specific factor. The variation ranges of all the factors cover the typical range in practice.

TABLE 2 Parameters for FEM analysis.

Material	γ (kN/m^3)	c' (kPa)	φ' (deg)	E(MPa)	ν
Embankment	18.5	10	26	20	0.3
Loam	19.1	20.5	27	35	0.3
Muddy clay	17.9	16.1	10	8	0.3
Sandy loam	1.84	11.9	20	25	0.3
Sandy clay	1.92	28.8	26.5	50	0.3
Silty sand	1.90	26.5	31.1	80	0.3
Gravel	1.78	3	30	30	0.3

Note: γ is the unit weight of soil; c' is the effective cohesion of soil; φ' is the effective friction angle; E is the Young's elastic modulus of soil; ν is the Poisson's ratio.

4 Measured and computed results

4.1 Performance of the geogrid-reinforced soil platform pile-supported embankment

The settlements of the pile and soil are illustrated in Figure 2A. Settlement plates measured the settlements. With the increase in the embankment height, the settlements of both the pile and soil increase, with the similar settlement trends. At the beginning of the embankment filling, the settlements of the pile and soil are quite small, and the settlement rate increases slowly, especially for the pile settlement. As the embankment reaches 2.5–3.0 m high, the settlement rate increases obviously, and the settlement rate of soil is larger than that of piles. The filling height of each step has a significant effect on the settlement rate (i.e., embankment height from 3.7 m to 5.7 m). Following the completion of embankment construction, settlement due to the gradual dissipation of excess pore water pressure accumulated during construction that continued for several months.

Figures 2B, C show the differential settlement and stress ratio of the pile and soil, respectively. The differential settlement obtained by subtracting the pile settlement from the foundation soil surface settlement reflects the deformation of GRSP. The stress ratio of pile to soil, defined as vertical stress acting on the pile head to that on the soil surface, was measured by earth pressure cells. The stress ratio reflects the load redistribution between the pile and soil due to deformation of the GRSP. At the beginning of embankment construction ($H < 1$ m), the settlement of the surrounding soil is small under the low embankment height. Consequently, the vertical stresses of the pile head and soil surface are almost identical, and the vertical stress concentration at the pile head is not obvious. When the embankment is higher than 1 m, soil settlement increases and capacity develops. In terms of the distinct difference of moduli of pile concrete and soil, the settlement of the pile is smaller, resulting in the pile–soil differential settlement. During this period, the effect of the GRSP is induced. The geogrid in the GRSP works as tensile nets between piles, transferring loads from soils to the piles through the tensile force in the geogrid and the friction force between the geogrid and platform gravel. With the embankment up to approximately 3.7 m high, the vertical stress on the soil surface increases slightly, whereas the pile–soil differential settlement and the vertical stress on the pile head increase significantly. During the following construction, the vertical stress on the soil surface and the pile–soil differential settlement is almost unchangeable, whereas the vertical stress on the pile head still increases remarkably. The vertical stress on the pile head became stable after the completion of

TABLE 3 Values of influencing factors of GRSP used.

Item	Parameter	Range of value
Gravel in GRSP	Elastic modulus (MPa)	15, 20, 25, 30*, 50, and 100
	Thickness (cm)	10, 20, 30, 40, and 50*
	Inner friction angle (deg)	10, 15, 20, 25, 30*, 35, and 40
Geogrid in GRSP	Tensile stiffness (kN/m)	600, 900, 1,125*, and 2.250
	Layers and placement	1 (middle), 2 (middle and upper)*, 2 (middle and lower), and 3 (middle, upper and lower)

*values used in the baseline case.

embankment construction, and the stable stress ratio of the pile and soil is 16.5, with the final pile–soil differential settlement of 114 mm.

According to the whole response process of the pile and soil in the construction of the embankment, including settlement and vertical stress, the GRSP plays an important role among the pile, foundation soil, and embankment filling. When the embankment height is less than 1 m, stresses on the pile and soil increase subtly, yet the pile–soil differential settlement is noticeable, which mainly results from the settlement of soil, and the existence of GRSP gravel keeps the surrounding soil carrying the load in the surface subsidence stage. When the embankment height reaches 3.7 m and the tensile force in the geogrid is stimulated gradually due to the increasing pile–soil differential settlement, the stiffness of the geogrid in GRSP limits the load applied on the soil surface and transfers the corresponding load to the pile head, which was reflected from the slight increase in soil stress and the prominent increase in pile stress. When the embankment was built from 3.7 m to 5.7 m, the pile and soil settle as an entirety and pile–soil differential settlement is nearly identical, revealing the stability of the interaction of pile and soil. The additional load at this stage is almost completely carried by pile-supported GRSP, as indicated by the slight increase in soil stress and prominent increase in pile stress, and the continuing soil settlement is mainly caused by the settlement of the pile. The comparison results of the pile–soil differential settlement and the vertical stresses on the pile head and soil surface are illustrated in Figures 2B, C, and the computed results are in a good agreement with the measured values.

Figure 3A displays the development processes of the stress ratio of pile to soil with different GRSP construction methods. The GRSP construction method has a significant influence on the developing mode of the stress ratio of the pile to soil and small influence on the final value of the stress ratio of the pile to soil, which is 17.0 and 16.5, respectively. The stress ratio of the pile to soil with the first type of the GRSP construction method is always larger than that of the second method, and the difference in the stress ratio of pile to soil between the two methods decreases in the whole construction process. With well-compacted GRSP (Method 1), the geogrid tensile force increases distinctly at the early stage and increases slowly at the later stage of embankment construction, owing to the plasticity of the geogrid under large tensile forces. In this study, the main method used for compacting the soil platform on the site is vibratory compaction, with engineering requirements stipulating that the compaction degree must exceed 90%. In contrast, the geogrid tensile force nearly linearly increases for the un-compacted GRSP case (Method 2) during construction.

Figure 3B shows the influences of the GRSP construction method on the horizontal displacement on the foundation surface at the embankment toe. It can be seen that during construction, the horizontal displacement is generally smaller for the well-compacted GRSP compared to the un-compacted GRSP. With the well-compacted GRSP, the final ground surface lateral displacements at the embankment toe are smaller, and the values of lateral displacement are 17.5 mm and 22.5 mm for the embankment with the compacted and un-compacted GRSP, respectively. The larger compaction of GRSP soil benefits both the reduction of embankment horizontal displacement and stability of embankment.

4.2 Load transfer mechanism of geogrid-reinforced compacted

The interactions among piles, foundation soil, embankment fill, and GRSP are schematically explained in Figure 4. Owing to the large stiffness difference between piles and foundation soil, the embankment fill between piles has a tendency to move downward under the self-weight of fill. The movement is partially constrained by the shear resistance (τ) from the fill overlying the piles. The shear resistance transfers the stresses in the embankment, which results in the reduction of the pressure ($\sigma_{a,s}$) acting on the surface of the GRSP between piles and the increase in the pressure ($\sigma_{a,p}$) acting on the surface of GRSP overlying piles. This load transfer mechanism is titled the "soil arching effect" (Terzaghi, 1943). The inner differential settlement in the embankment induced by the differential settlement between the pile and soil varies at different levels of embankment height. To a certain height (h_s), the inner differential settlement is absent due to the shear resistance (τ) from the fill overlying the piles, and a plane of equal settlement (PES) exists (Terzaghi, 1936). In addition to the effect of geosynthetics in GRSP, the soil in GRSP has influences on the load mechanism as well. As a result of the penetration of the pile head into the GRSP soil (i.e., gravel), the GRSP soil partially transfers to the surrounding soil of pile, ensuring that upper loads act on the foundation soil, and the contact surface force between geosynthetics and soil in GRSP is influenced, which affects the tensile force in geosynthetics. In summary, the characteristics of GRSP have significant influences on the load transfer mechanism, including stress concentration on the pile head, soil arching effect of the embankment, tensioned membrane of

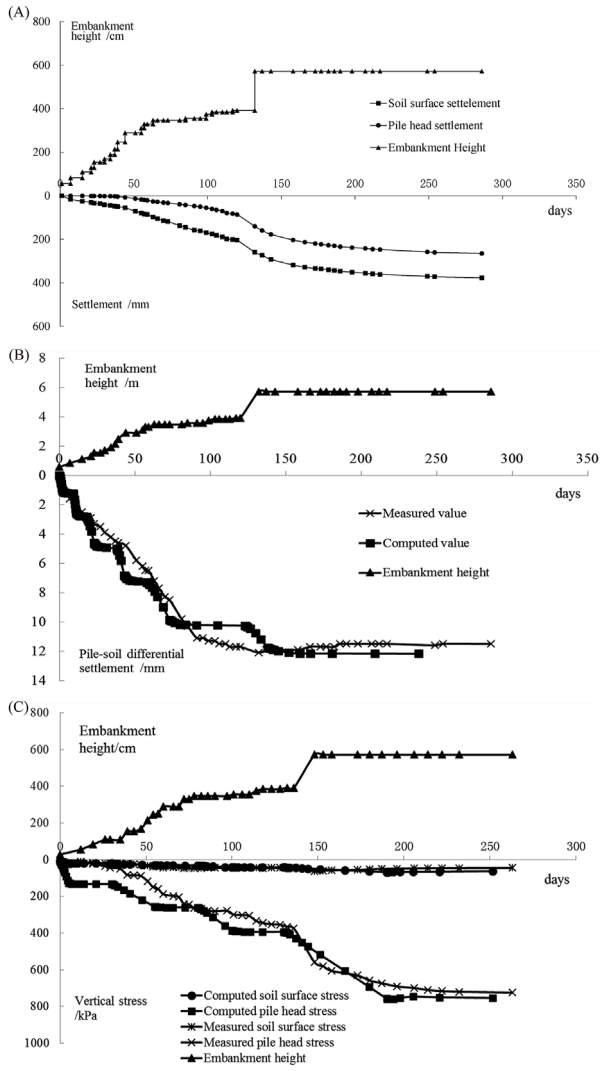

FIGURE 2
(A) Measured settlement of the pile head and soil surface. **(B)** Measured and computed differential settlement of the pile head and soil surface. **(C)** Measured and computed pressure acted on the pile head and soil surface.

geosynthetics, and differential settlement between piles and soil. The effects of GRSP modulus, thickness, shear resistance, and geosynthetic stiffness, layers, and placement will be investigated.

Based on the load transfer mechanism, several coefficients are introduced to discuss the effects of GRSP on the soil arching effect of the embankment, tensioned membrane effect of geosynthetics, and stress concentration of pile, including i) the stress concentration ratio of the pile head to the soil surface (n), which reflects the final load-sharing proportion between the pile and soil due to the soil arching, tensioned membrane effect, and penetration resistance of GRSP; ii) the degree of the soil arching effect (ρ_a), which reflects the stress reduction at the bottom of the embankment fill between piles due to soil arching; iii) the degree of composite effects of soil arching and tensioned membrane ($\rho_{a,m}$), which reflects the stress reduction at the foundation soil surface due to both soil arching and tensioned membrane effects; iv) the degree of the tensioned membrane (ρ_m), which reflects the stress reduction at the foundation soil surface due to the tensioned membrane effect.

The stress concentration ratio of the pile head to the soil surface is defined as Equation 1

$$n = \frac{\sigma_{am,p}}{\sigma_{am,s}}, \tag{1}$$

where $\sigma_{am,p}$ is the applied pressure on the pile head and $\sigma_{am,s}$ is the applied pressure on the soil surface between piles.

The degree of the soil arching effect is given by Equation 2 (as proposed in (McNulty, 1965))

$$\rho_a = \frac{\sigma_{a,s}}{\gamma_f H_f + q_0}, \tag{2}$$

where ρ_a is the soil arching ratio; $\rho_a = 0$ represents the complete soil arching effect, while $\rho_a = 1$ represents no soil arching; $\sigma_{a,s}$ is the applied pressure on the top of the trapdoor in Terzaghi or McNulty's studies (the GRSP surface between piles in this study); γ_f is the unit weight of the embankment fill; H_f is the height of the embankment; and q_0 is the surcharge on the embankment. Furthermore, the degree of load transfer from soil to pile through the soil arching effect can be quantified with $(1\text{-}\rho_a)$.

The degree of composite effects of soil arching and tensioned membrane is given by Equation 3

$$\rho_{a,m} = \frac{\sigma_{am,s}}{\gamma_f H_f + \gamma_c H_c + q_0}, \tag{3}$$

where $\rho_{a,m}$ is the composite effect ratio of soil arching and tensioned membrane; $\rho_{a,m} = 0$ represents the load carried by piles completely, while $\rho_{a,m} = 1$ represents no soil arching and tensioned membrane effects; γ_c is the unit weight of GRSP soil; H_c is the thickness of GRSP. Furthermore, the degree of load transfer from soil to pile through the soil arching and tensioned membrane effects can be quantified with $(1\text{-}\rho_{a,m})$.

The degree of tensioned membrane is defined as Equation 4

$$\rho_m = \rho_a - \rho_{a,m}, \tag{4}$$

where ρ_m is the tensioned membrane ratio, which can quantify the degree of load transfer from the soil to pile through the tension membrane effect and $\rho_m = 1$ represents the complete tensioned membrane effect, while $\rho_a = 0$ represents no tensioned membrane effect.

4.3 Influences of the GRSP modulus on stresses and settlements of pile and soil

4.3.1 Influences of the GRSP modulus on stresses

The degree of the stress concentration from soil to pile is typically evaluated with the stress concentration ratio of the pile head to soil surface (n). The higher the n, the additional loads are transferred to the pile from soil. As shown in Figure 5A, n increases with the increase in the elastic modulus of the GRSP material. As the elastic modulus increases from 15 MPa to 100 MPa, n increases from 10.1 to 18.6. As the elastic modulus of the GRSP increases, its deformation resistance improves, allowing more load

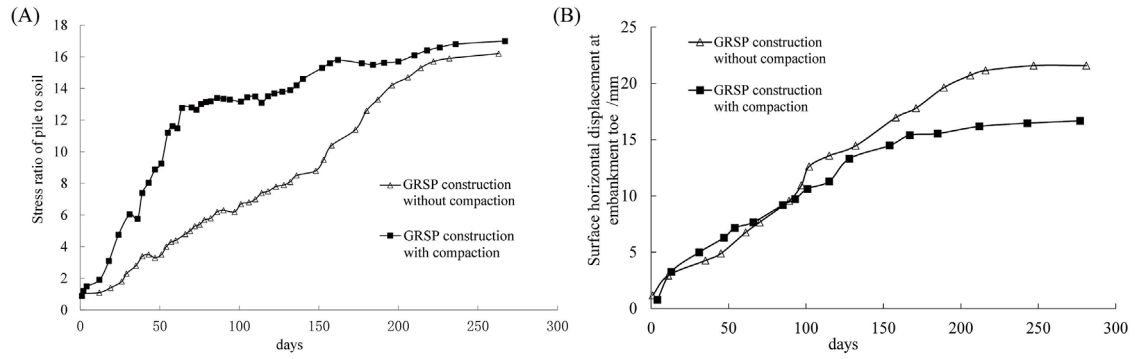

FIGURE 3
(A) Measured stress concentration of the pile and soil with different GRSPs. **(B)** Measured lateral displacement of the ground surface at the embankment toe.

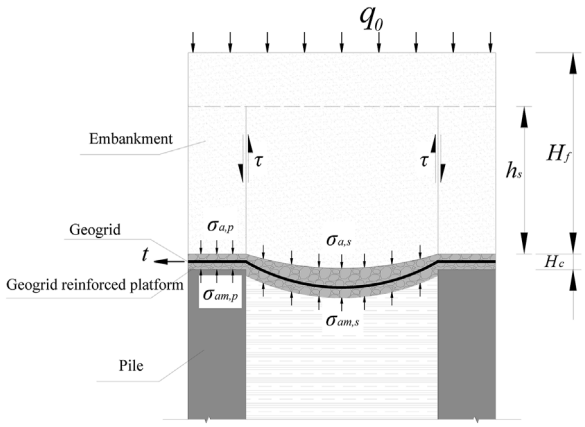

FIGURE 4
Load transfer mechanisms of GRSP in the pile-supported embankment.

to be effectively transferred to the piles, with the GRSP functioning as a deformed beam between the piles.

Except for the stress concentration ratio, the load transfer mechanisms are affected at different degrees owing to the variety of the GRSP modulus, as presented in Figure 5B. With the increase in the GRSP material modulus, the soil arching ratio (ρ_a) and tensioned membrane ratio (ρ_m) increase, while the composite soil arching and tensioned membrane ratio ($\rho_{a,m}$) decrease. As the elastic modulus increases from 15 MPa to 100 MPa, ρ_a increases from 0.75 to 0.84, ρ_m increases from 0.33 to 0.58, and $\rho_{a,m}$ decreases from 0.42 to 0.25. The increase in ρ_a reflects the weakening of the soil arching effect in the embankment, which results in less loads transferred to the pile, but the corresponding increase in ρ_m implies the enhancement of the tensioned membrane effect of GRSP, which leads to additional loads transferred to the pile. The two opposite tendencies mutually affect the load transfer between the pile and soil. Then, the decrease in $\rho_{a,m}$ also shows the composite effect of soil arching, and tensioned membrane is strengthened, which results in the increase in pile–soil stress concentration ratio and loads acted on pile, as mentioned above. Therefore, the increase in the GRSP modulus helps to transfer additional loads to pile heads. Furthermore, the influence of the GRSP modulus on the tensioned membrane effect is more notable than that on the soil arching effect. The increases in ρ_m and ρ_a are 77.1% and 12%, respectively, as the elastic modulus increases from 15 MPa to 100 MPa.

4.3.2 Influences of the GRSP modulus on settlements

As shown in Figure 5C, the elastic modulus of GRSP affects the settlements of the pile and soil, including the differential settlement of the pile and soil, the settlement of the embankment surface, the height of the plane of equal settlement (PES) h_s in the embankment, and the settlement of PES. The settlement results of different moduli are normalized based on the case of the GRSP modulus of 15 MPa. All the settlements decrease with the increase in the GRSP modulus. Due to the increase in the GRSP modulus, the deformation of GRSP decreases, causing reduction in pile–soil differential settlement. The decrease in the differential settlement of pile and soil is prominent, and the maximum reduction is estimated to be 24% within the variation range of the GRSP modulus. The settlements of the embankment surface and PES also decrease, with the maximum reductions of 9.2% and 9.8%, respectively. The influence of the GRSP modulus on the height of PES h_s is relatively small, especially when it exceeds 25 MPa, with a maximum reduction of 5.1% in this analysis. The lowering of the height of PES h_s demonstrates the decrease in the inner differential settlement in the embankment and the weakening of the soil arching effect, as illustrated in Figure 5B.

4.4 Influences of GRSP thickness on stresses and settlements of pile and soil

4.4.1 Influences of GRSP thickness on stresses

Figure 6A presents the stress concentration ratio of the pile head to the soil surface versus the thickness of GRSP. Clearly, the stress concentration ratio of pile to soil linearly increases with an increase in the thickness of GRSP in this analysis. In other words, the stress concentration ratio of pile to soil increases with an increase in the thickness of GRSP. This result can be explained that when

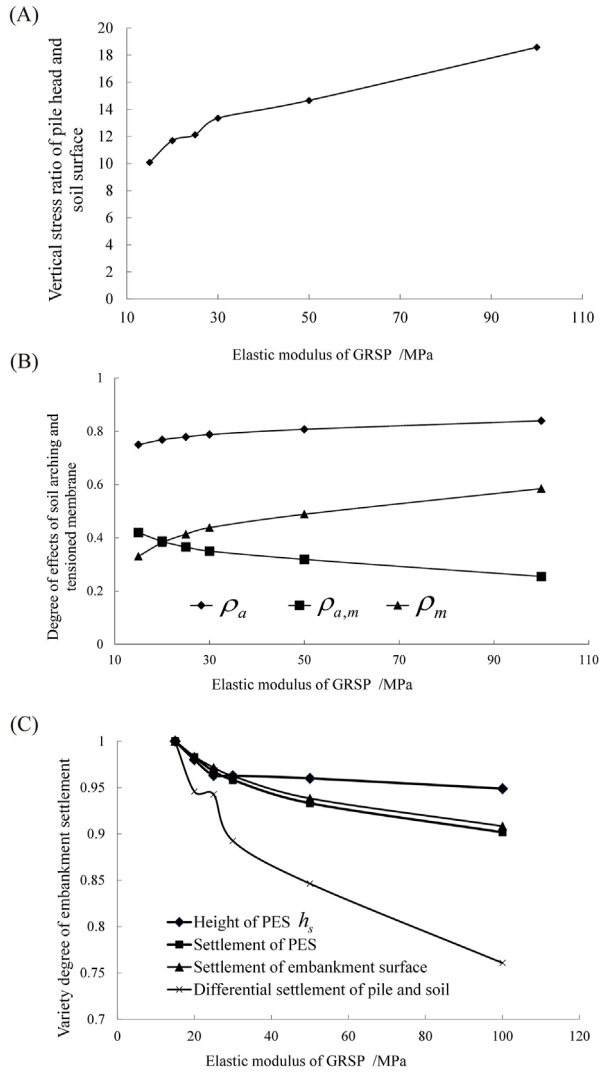

FIGURE 5
(A) Influence of the elastic modulus of GRSP on the stress concentration ratio of pile to soil (*n*). **(B)** Influence of the elastic modulus of GRSP on the effects of soil arching and tensioned membrane. **(C)** Influence of the elastic modulus of GRSP on embankment settlements.

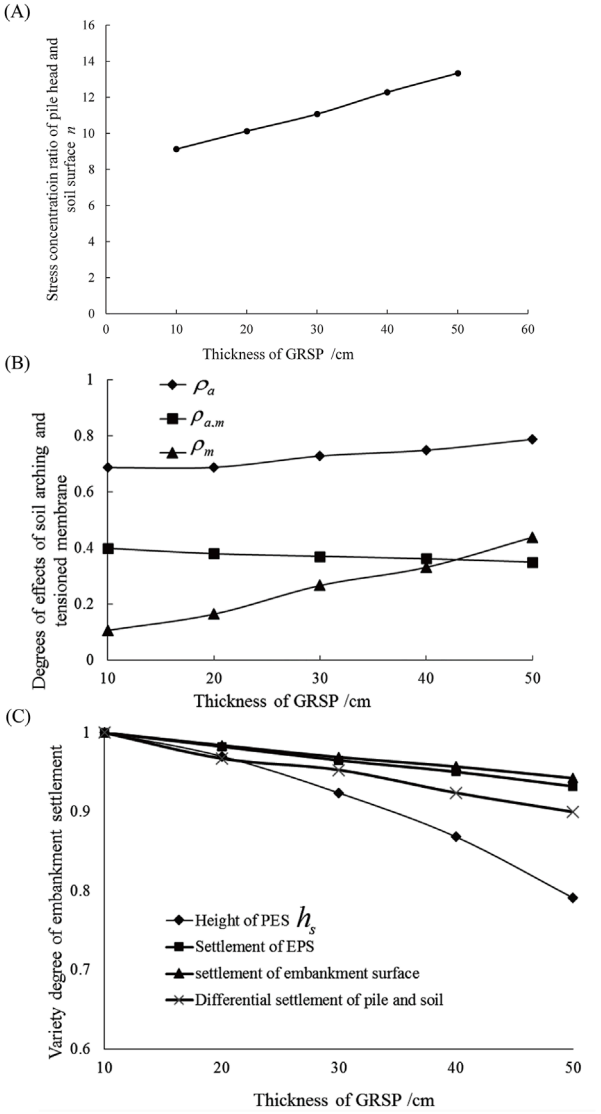

FIGURE 6
(A) Influence of the thickness of GRSP on the stress concentration ratio of pile to soil (*n*). **(B)** Influence of the thickness of GRSP on the effects of soil arching and tensioned membrane. **(C)** Influence of the thickness of GRSP on embankment settlements.

the GRSP is thicker, the deformation resistance of GRSP can be strengthened, which is similar to the increase in the GRSP modulus mentioned above, and more stresses can be transferred to piles through GRSP. As the thickness increases from 10 cm to 50 cm, the stress concentration ratio increases by 46.5% from 9.1 to 13.4.

The different degrees of effects of soil arching and tensioned membrane are plotted against the GRSP thickness in Figure 6B. Consistent with the stress concentration ratio, the thicker the GRSP, the higher the soil arching ratio (ρ_a) and tensioned membrane ratio (ρ_m). However, the composite soil arching and tensioned membrane ratio ($\rho_{a,m}$) decreases with an increase in GRSP thickness. As the GRSP thickness increases from 10 cm to 50 cm, ρa increases from 0.69 to 0.79; ρm increases from 0.11 to 0.44, and $\rho_{a,m}$ decreases from 0.40 to 0.35. The increase in ρ_a reflects the decreases in the soil arching effect in the embankment, which causes less loads transferred to the pile, but the correlating increase in ρ_m shows the enhancement of the tensioned membrane effect of GRSP, which results in additional loads transferred to the pile. The two opposite tendencies affect the load transfer between the pile and soil together. The ultimate adjustments of soil arching and tensioned membrane induce additional loads applied to piles, which is reflected by the decrease in $\rho_{a,m}$. Therefore, the increase in GRSP thickness benefits in transfer of additional loads to pile heads. Moreover, ρ_a, ρ_m, and $\rho_{a,m}$ nearly linearly vary with the increase in GRSP thickness, and the influence on the tensioned membrane effect is more pronounceable than that on the soil arching effect. The increases in ρ_m and ρ_a are 0.33 and 0.10, respectively, as the elastic modulus increases from 10 cm to 50 cm.

4.4.2 Influence of GRSP thickness on settlements

Figure 6C demonstrates the influence of GRSP thickness on the settlements of pile and soil, including the differential settlement of pile and soil, the settlement of the embankment surface, the height of the plane of equal settlement (PES) h_s in the embankment, and the settlement of PES. The settlement results of different thicknesses are normalized based on the case of 10-cm-thick GRSP. With the increase in GRSP thickness, the settlements of pile and soil all decrease at different rates. The influence on the height of PES h_s is greater than that of the other settlements, with a maximum reduction of 20.9% within the variation range of the GRSP thickness in this analysis. The enhanced deformation resistance of GRSP resulting from the increase of thickness causes the reduction of h_s and the improvement of the stress concentration ratio of pile and soil, as discussed in the previous section. The lowering of the height of PES h_s demonstrates the reduction in inner differential settlement in the embankment and the weakening of soil arching effect, as illustrated in Figure 6B. Additionally, on account of the different varying rates of the height of PES h_s and soil arching ratio ρ_a within the varying range of the GRSP thickness, the increasing compression of GRSP with the increase in the thickness also plays an important role on the reduction rate of h_s. The differential settlement of pile and soil also decreases with the increase in the GRSP thickness, with a maximum reduction of 10% in this analysis. The influence of the GRSP modulus on the settlement of the embankment surface and the settlement of PES is relatively small, with the maximum reductions of 5.7% and 6.8%, respectively.

4.5 Influence of GRSP shear resistance on stresses and settlements of pile and soil

4.5.1 Influence of GRSP shear resistance on stresses

The shear resistance of the GRSP material (i.e., friction angle and cohesion) is expected to affect the performance of the pile and soil. In practical applications, gravel or sand is commonly used as the GRSP material due to its effectiveness in dissipating excess pore water pressure within the soil. Consequently, the variation in cohesion is minimal, and the effect of GRSP material cohesion is disregarded in this analysis. However, the influence of the friction angle of the GRSP material is analyzed as below.

As shown in Figure 7A, the friction angle of the GRSP material influences the stress concentration ratio of the pile head to the soil surface. Noticeably, the stress concentration ratio of pile to soil linearly increases with an increase in the friction angle of the GRSP material. In other words, it is effective to increase the stress concentration ratio of pile to soil when the friction angle of the GRSP material increases. The results can be explained by the fact that the larger friction angle induced the higher shear resistance and more loads were transferred to the pile head from soil, which is the same as that of the increase in GRSP modulus or thickness. When the friction angle increases from 10°to 40°, the stress concentration ratio increases from 10.1 to 14.7.

The different degrees of effects of soil arching and tensioned membrane versus friction angle are illustrated in Figure 7B. Consistent with the stress concentration ratio, with the increase in the friction angle, both the soil arching ratio (ρ_a) and the tensioned membrane ratio (ρ_m) also increase. Nevertheless, the increased friction angle induces the decrease in composite soil arching and tensioned membrane ratio ($\rho_{a,m}$). As the GRSP friction angle increases from 10° to 40°, ρ_a increases from 0.77 to 0.79, ρ_m increases from 0.03 to 0.50, and $\rho_{a,m}$ decreases from 0.43 to 0.34. The increase in ρ_a reflects the decrease in the soil arching effect, which causes less loads transferred to the pile, but the correlating increase in ρ_m shows the enhancement of the tensioned membrane effect of GRSP, which results in additional loads transferred to the pile. The two opposite tendencies affect the load transferring between the pile and soil, and the final adjustment of the two effects induced additional loads applied on the pile, which is reflected by the decrease in $\rho_{a,m}$. Hence, the increase in the GRSP friction angle

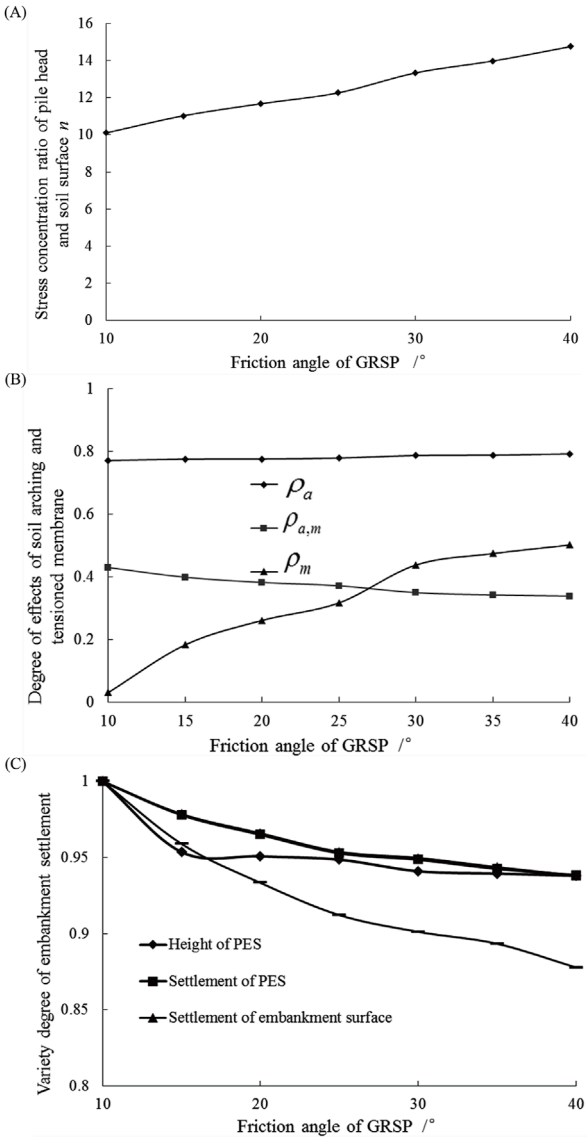

FIGURE 7
(A) Influence of friction angles of GRSP on the stress concentration ratio of pile to soil (*n*). **(B)** Influence of friction angles of GRSP on the effects of soil arching and tensioned membrane. **(C)** Influence of friction angles of GRSP on embankment settlements.

displays the benefit for transferring additional loads to the pile. Furthermore, the influence on the tensioned membrane effect is more noticeable than that on the soil arching effect. The increases in ρ_m and ρ_a are approximately 0.47 and 0.02, respectively, as the angle friction increases from 10° to 40°.

As shown in Figure 7C, the friction angle of the GRSP material has effects on the settlements of the pile and soil, including the differential settlement of the pile and soil, the settlement of the embankment surface, the height of the plane of equal settlement (PES) h_s in the embankment, and the settlement of PES. The settlement results of different friction angles are normalized based on the case of the 10° GRSP friction angle. All the settlements decrease with the increase in the friction angle of GRSP. Due to the increase in the GRSP friction angle, the shear resistance of GRSP increases, causing the reduction in the shear deformation of GRSP and the pile–soil differential settlement. The decrease in the differential settlement of pile and soil is apparent, with the maximum reduction estimated at 12.2% within the variation range of the GRSP friction angle. The settlements of embankment surface and PES also decrease, with the maximum reductions of 6.18% and 6.15%, respectively. The reduction in the height of PES h_s is maximum 6.19% in this analysis, and the influence is even smaller as the friction angle of GRSP exceeds 15°. The lowering of the height of PES h_s presented the decrease in inner differential settlement in embankment, which is consistent with the weakening of the soil arching effect, as illustrated in Figure 7B.

4.6 Influence of geogrid tensile stiffness on stresses and settlement of pile and soil

4.6.1 Influence of geogrid tensile stiffness on stresses

Figure 8A demonstrates the stress concentration ratio of the pile head and soil surface versus the tensile stiffness of the geogrid. Clearly, the stress concentration ratio of the pile to soil increased significantly with an increase in the tensile stiffness of the geogrid in GRSP. In other words, the stress concentration ratio of the pile to soil can be improved by increasing the tensile stiffness of the geogrid. This result is in good agreement with the findings obtained by Han and Gabr (2002). It can be explained that when the tensile stiffness of the geogrid is higher, the deformation resistance of the GRSP is enhanced. This effect is similar to the impact of other physical or mechanical parameters of the GRSP mentioned earlier, such as increased elastic modulus, thickness, and shear resistance, enabling greater load transfer to the piles through the GRSP between them. As the tensile stiffness increases from 300 kN/m to 2,250 kN/m, the stress concentration ratio increases by 58.9% from 10.4 to 16.5.

The influences of geogrid tensile stiffness on the effects of soil arching and tensioned membrane are plotted in Figure 8B. Consistent with the stress concentration ratio, the higher the tensile stiffness of the geogrid, the larger the soil arching ratio (ρ_a) and tensioned membrane ratio (ρ_m). However, the composite soil arching and tensioned membrane ratio ($\rho_{a,m}$) decreases with an increase in the geogrid tensile stiffness. As the geogrid tensile stiffness increases from 300 kN/m to 2,250 kN/m, ρ_a increases from 0.73 to 0.83, ρ_m increases from 0.32 to 0.48, and $\rho_{a,m}$ decreases from 0.40 to 0.32. The increase in ρ_a reflects the weakening of the soil arching effect in the embankment, causing less loads to be transferred to the pile, but the correlating increase in ρ_m showed the enhancement of the tensioned membrane effect of GRSP, resulting in additional loads being transferred to the pile. The two opposite tendencies affected the load transfer between the pile and soil mutually. The crucial adjustment of soil arching and tensioned membrane induces additional loads applied on the pile, which is reflected by the decrease in $\rho_{a,m}$. Therefore, the increase in geogrid tensile stiffness greatly benefits the transfer of additional loads to pile heads. Moreover, the ρ_a, ρm, and $\rho_{a,m}$ vary at different rates, and the influence on the tensioned membrane effect was more pronounceable than that on the soil arching effect. The increases in

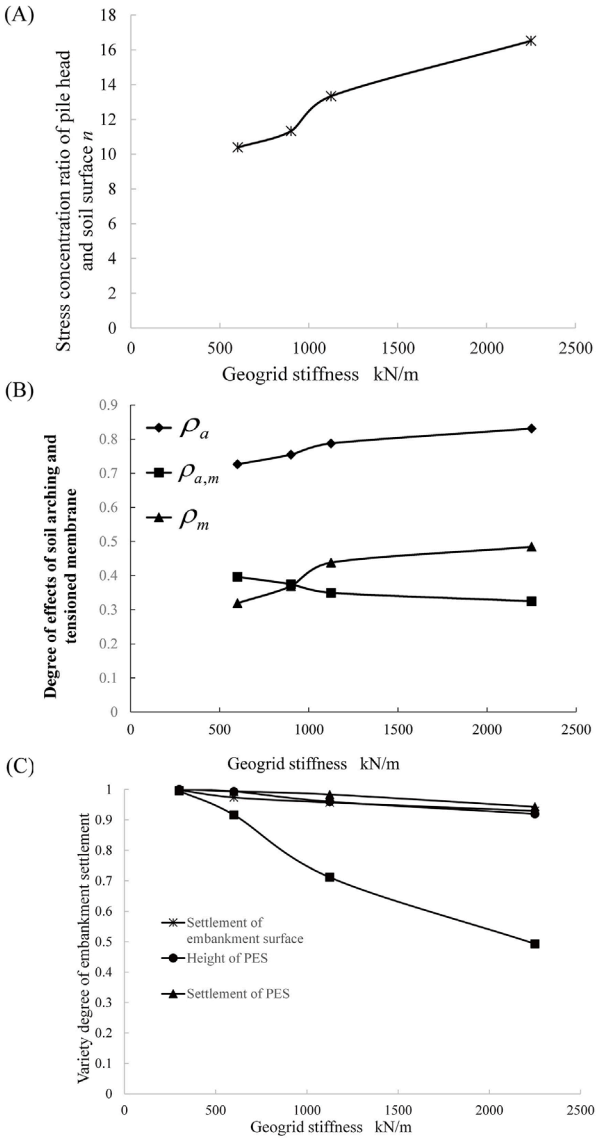

FIGURE 8
(A) Influence of tensile stiffness of the geogrid on the stress concentration ratio of pile to soil (*n*). **(B)** Influence of tensile stiffness of the geogrid on the effects of soil arching and tensioned membrane. **(C)** Influence of tensile stiffness of the geogrid on embankment settlements.

ρ_m and ρ_a are approximately 0.17 and 0.1, respectively, as the geogrid tensile stiffness increases from 300 kN/m to 2,250 kN/m.

4.6.2 Influence of geogrid tensile stiffness on settlements

As illustrated in Figure 8C, the tensile stiffness of the geogrid also has an influence on the settlements of pile and soil, including the differential settlement of pile and soil, the settlement of the embankment surface, the height of the plane of equal settlement (PES) h_s in the embankment, and the settlement of PES. The settlement results of different tensile stiffness are normalized based on the case of 300 kN/m tensile stiffness of the geogrid. All the settlements decrease with the increase in the geogrid tensile stiffness. Due to the increase in tensile stiffness, the deformation resistance of GRSP increases, which induces the reduction of the deformation of GRSP and the pile–soil differential settlement. The decrease in the differential settlement of pile and soil is significant, with the maximum reduction estimated to be 50.5% within the variation range of the geogrid tensile stiffness. The settlements of embankment surface and PES also decrease, with the maximum reductions of 6.9% and 5.7%, respectively. The reduction of the height of PES h_s is maximum 8.1% in this analysis. The lowering of the height of PES h_s shows the decrease in the inner differential settlement in the embankment and agrees well with the weakening of the soil arching effect as discussed earlier.

4.7 Influences of geogrid layers and placement on stresses and settlements of pile and soil

4.7.1 Influence of geogrid layers and placement on stresses

Figure 9A presents the stress concentration ratio of the pile head to the soil surface versus the geogrid layers and placement. The stress concentration ratio of the pile to soil increases with the increase in the geogrid layers and the lowering placement of the geogrid in GRSP. In other words, the stress concentration ratio of the pile to soil is strengthened by increasing the layers of the geogrid and lowering the placement elevation of the geogrid in GRSP. These results can be explained by the fact that when the geogrid layers increase or the placement elevation of geogrid reduce, the deformation resistance of GRSP under pile penetration is strengthened, which was similar to the increase in the geogrid tensile stiffness, and additional loads can be transferred to piles through GRSP between piles. As the geogrid layers increase from single layer to triple layers, the stress concentration ratio increases by 11% from 12.8 to 14.2. When one of the geogrid layers is shifted from the top of GRSP to the bottom in the double layer cases, the stress concentration ratio increases slightly from 13.3 to 13.6 at an approximately 2.2% increasing rate.

The different degrees of effects of soil arching and tensioned membrane versus geogrid layers and placement are illustrated in Figure 9B. Consistent with the stress concentration ratio, the more the geogrid layers, the larger the soil arching ratio (ρ_a) and tensioned membrane ratio (ρ_m). However, the composite soil arching and tensioned membrane ratio ($\rho_{a,m}$) decreases with an increase in geogrid layers. As the geogrid layers increase from single layer to triple layers, the increase in ρ_a is slight from 0.77 to 0.78, ρ_m increases distinctly from 0.26 to 0.45, and $\rho_{a,m}$ decreases from 0.42 to 0.34. The slight increase in ρ_a reflects the weakening of the soil arching effect in the embankment owing to the increase in geogrid layers, whereas the corresponding increase in ρ_m shows the enhancement of the tensioned membrane effect of GRSP, which results in additional loads transferred to the pile. With the mutual effects of soil arching and tensioned membrane, the additional loads are transferred to piles, which were reflected by the decrease in

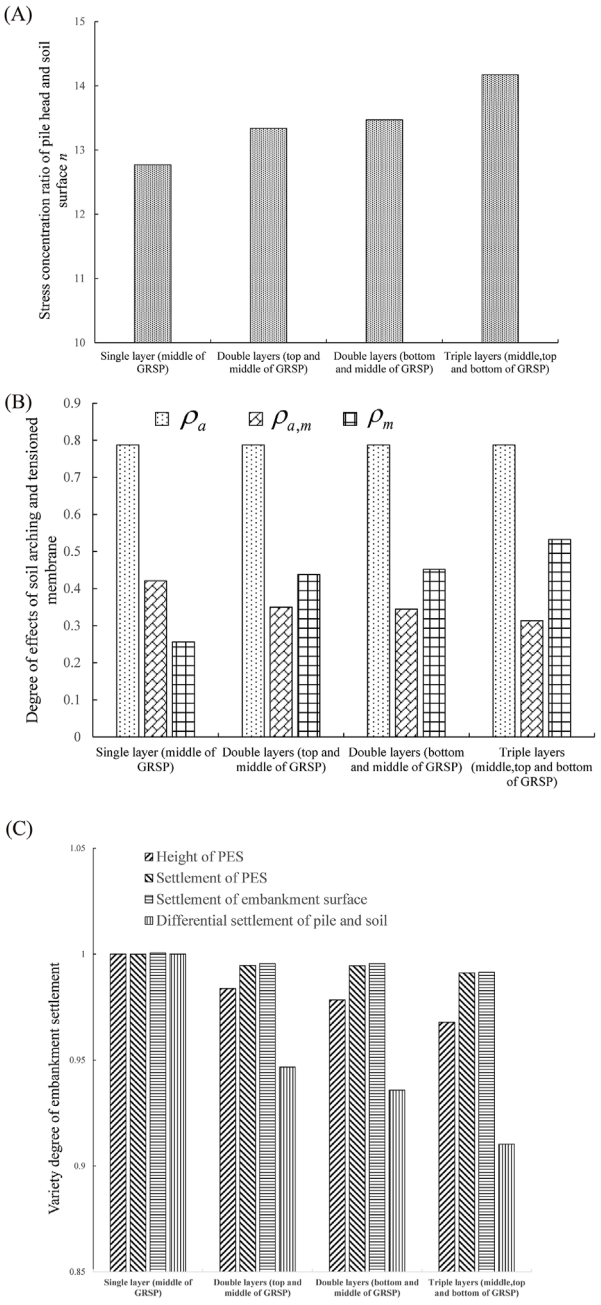

FIGURE 9
(A) Influence of layer and placement of the geogrid in GRSP on the stress concentration ratio of pile to soil (*n*). **(B)** Influence of the layer and placement of the geogrid in GRSP on the effects of soil arching and tensioned membrane. **(C)** Influence of the layer and placement of the geogrid in GRSP on embankment settlements.

$\rho_{a,m}$ directly. Therefore, the increase in geogrid layers benefits the transfer of the loads to pile heads. Moreover, the placement of the geogrid with the same layers influences the soil arching and tensioned membrane as well at a certain degree. As one of the geogrid layer is shifted from the top of GRSP to the bottom in the double layer cases, ρ_a inappreciably increases from 0.787 to 0.788, ρ_m increases distinctly from 0.44 to 0.45, and $\rho_{a,m}$ decreases from 0.65 to 0.64 in this analysis. Hence, the influences of the placement of the geogrid on the effects of soil arching and tensioned membrane are practically ignorable.

4.7.2 Influence of geogrid layers and placement on settlements of pile and soil

As shown in Figure 9C, the layers and placement of the geogrid in GRSP affect the settlements of pile and soil, including the differential settlement of the pile and soil, the settlement of the embankment surface, the height of the plane of equal settlement (PES) h_s in the embankment, and the settlement of the PES. The settlement results of different layer quantity and placement are normalized based on the case of the single layer of the geogrid in the middle of GRSP. All the settlements decrease at different degrees, with the increase in the quantity of the geogrid layer. Due to the increase in geogrid layers, the deformation resistance of GRSP increases, resulting in the reduction in the deformation of GRSP and the pile–soil differential settlement. The decrease in the differential settlement of the pile and soil is apparent, with the maximum reduction estimated to be 9.0% within the variation range of the geogrid in this analysis. The settlements of the embankment surface and PES also decrease slightly, with the maximum reductions of 0.91% and 0.88%, respectively. The reduction in the height of PES h_s is maximum 3.2% in this analysis. The lowering of the height of PES h_s results in the reduction of inner differential settlement in the embankment, which is consistent with the weakening of the soil arching effect, as illustrated in Figure 9B. As for the influences of geogrid placement, the settlements of soil and piles are affected negligibly. As one of the geogrid layer is shifted from the top of GRSP to the bottom in the double layer cases, the pile–soil differential settlement slightly decreases from 0.95 to 0.93, the height of PES h_s decreases inappreciably from 0.98 to 0.97, and the settlements of the embankment surface and PES are almost unchanged, which are approximately 0.995 and 0.994, respectively.

5 Discussion

The influences of various factors of GRSP on the stress concentration ratio of pile to soil, soil arching effect, tensioned membrane effect, differential settlement of pile and soil, settlement of embankment surface, and height of PES in embankment and its settlement are summarized below.

According to the definitions of the composite ratio of soil arching and tensioned membrane effects ($\rho_{a,m}$), the degree of load transfer from soil to pile through the two effects can be quantified with (1-$\rho_{a,m}$). In the 22 cases of numerical computations, the values of 1-$\rho_{a,m}$ are approximately 0.55–0.75, which reflects that most load of the embankment is transferred to the piles, and the soil arching and tensioned membrane effects are effective and efficient to reduce the load applied on ground soil. However, the parametric studies also

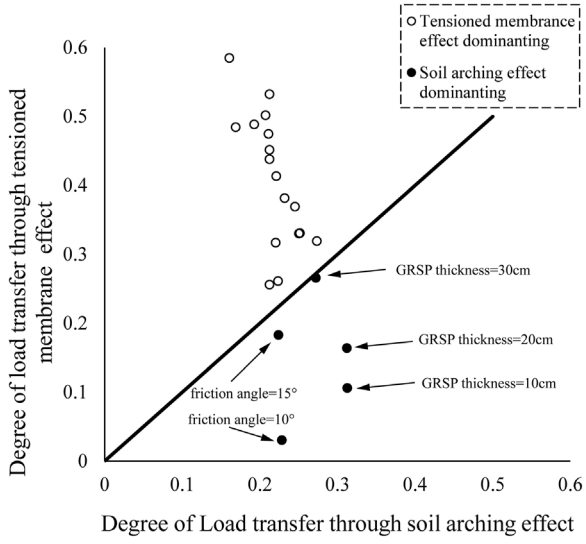

FIGURE 10
Load transfer degrees with the effects of soil arching and tensioned membrane.

reveal that the major role of load transfer is varied in different cases. Similarly to (1-$\rho_{a,m}$), the degree of load transfer through the soil arching effect and tensioned membrane effect can be quantified with (1-ρ_a) and ρ_m, respectively. Figure 10 presents the degree of load transfer through the tensioned membrane effect ρ_m versus the degree of load transfer through the soil arching effect (1-ρ_a), and the straight line in figure means the equivalent efficiency of the two effects in load transfer. Clearly, the tensioned membrane effect of GRSP mostly plays the principal role in the transfer of load from soil to piles in the 22 computation cases. The degrees of load transfer through the soil arching effect are approximately 20%–25% mostly, and the degrees of load transfer through the tensioned membrane effect are mainly larger than 30%, with some cases exceeding 50%. However, in the five cases located to the right of the straight line, it is observed that smaller friction angles and reduced GRSP thickness emphasize the dominant role of the soil arching effect in load transfer. Overall, except in the scenarios characterized by smaller friction angles and thinner GRSP layers, the tensioned membrane effect of the GRSP generally plays a more significant role in transferring loads from the embankment soil to the piles.

Various factors of the GRSP, including elastic modulus, thickness, friction angle, tensile stiffness, and the number of geogrid layers, all have positive effects. Increasing these factors facilitates greater load transfer from the soil to the piles and reduces embankment settlement. However, increases in various GRSP factors lead to different load transfer processes. For example, the increase in these influencing factors shows negative effects on soil arching and positive effects on the tensioned membrane effect. The influencing degree of each influencing factor has been introduced to evaluate the variation degree of investigated performance parameters, such as the stress concentration ratio of pile and soil, soil arching effect, tensioned membrane effect, differential settlement of pile and soil, settlement of embankment surface, and the height of PES in the embankment and its settlement. The influencing degree

TABLE 4 Degrees of influencing factors.

GRSP factor	n	ρ_a	ρ_m	$\rho_{a,m}$	S_d	S_e	h_s	S_{PES}
Modulus	63.4	11.4	58.0	47.3	26.6	9.5	5.3	10.3
Thickness	31.7	13.5	117.1	13.3	10.6	5.9	22.9	7.0
Friction angle	37.3	2.7	149.7	24.5	13.2	6.4	6.5	6.4
Tensile stiffness of the geogrid	47.6	13.8	41.0	19.7	64.5	7.1	8.3	5.8
Layers of the geogrid	10.4	0	67.6	29.9	9.4	0.9	3.3	0.9
Placement of the geogrid	1.0	0	3.0	1.5	1.2	0	0.5	0

Note: n is the stress concentration ratio of pile to soil; ρ_a is the soil arching ratio; ρ_m is the tensioned membrane ratio; $\rho_{a,m}$ is the composite ratio of soil arching and tensioned membrane; S_d is the differential settlement of soil and pile; S_e is the settlement of embankment surface; h_s is the height of plane of equal settlement (PES) in embankment; S_{PES} is the settlement of PES.

is defined as the ratio of the maximum variation of the performance parameter to the mean value of the performance parameter. As an example, the stress concentration ratios of pile to soil for the GRSP elastic modulus equal to 15, 20, 25, 30, 50, and 100 MPa are 10.1, 11.7, 12.1, 13.5, 14.7, and 18.6, respectively. The maximum variation of the stress concentration ratio of pile to soil within the variation range in this analysis is 18.6–10.1 = 8.5, and the mean value of the stress concentration ratio of the pile and soil is (10.1+11.7+12.1+13.5+14.7+18.6)/6 = 13.45. Hence, the degree of influence of the GRSP elastic modulus on the stress concentration ratio of the pile to soil is calculated as (8.5/13.45)×100% = 63.2%. The calculated degree of influence for each factor on each investigated performance parameter is listed in Table 4.

According to the results shown in Table 4, the elastic modulus of GRSP has significant influences on the performance of the pile-supported embankment, especially on the stress concentration ratio of pile to soil, the composite soil arching and tensioned membrane ratio, the settlement of the embankment surface, and PES. The thickness of GRSP affected the height of PES and tensioned membrane ratio notably, compared to other factors, and the influence of the larger compression value for thicker GRSP should be taken into account. The friction angle of the GRSP material influences the tensioned membrane ratio significantly as well. The tensile stiffness of the geogrid has a significant impact on the soil arching ratio and the differential settlement of soil and pile. The influence of the geogrid layer on the tensioned membrane ratio is noticeable. The influence of geogrid placement on the performance of the pile-supported embankment is practically negligible. The settlement of the embankment surface and the stress concentration ratio of pile to soil are the important controlling indexes in practice; thus, the elastic modulus, tensile stiffness, and friction angle can be considered the three most important design parameters among the discussed influencing factors.

6 Conclusion

Based on the field monitoring and numerical parametric studies on the influences of GRSP on the performances of pile-supported embankment, the following conclusions can be drawn:

(1) By comparing field observation results of the embankment sections with different GRSPs, it is found that the compaction of the GRSP material affects the developing process of the stress concentration ratio of pile to soil, as well as the lateral displacement of the embankment. If the GRSP material is well compacted, the stress concentration ratio of the pile to soil increases distinctly at the early stage of embankment construction, and the lateral displacement becomes smaller compared to the un-compacted case.

(2) In reference to the definition of the soil arching ratio (ρ_a), the composite ratio of soil arching and tensioned membrane ($\rho_{a,m}$) and the tensioned membrane ratio of GRSP (ρ_m) are introduced to quantify the loading effect of GRSP, according to the load transfer mechanisms of the pile-supported embankment.

(3) A number of factors of GRSP influence not only the results of load transfer between pile and soil (i.e., the stress concentration ratio of pile to soil and the settlement of embankment surface) but also the process of load transfer (i.e., soil arching ratio, tensioned membrane ratio, and the differential settlement of pile and soil). The soil arching and tensioned membrane effects effectively reduce the load applied on the ground soil, with the tensioned membrane effect of GRSP typically playing a predominant role in transferring loads from soil to piles compared to the soil arching effect.

(4) With an increase in the GRSP factor (elastic modulus, thickness, friction angle, tensile stiffness, and layers of the geogrid), the load transferred to piles increases, and all the corresponding settlements decrease at different degrees. However, the soil arching effect in the embankment and the tensioned membrane effect in the GRSP exhibit opposite trends: the soil arching effect is diminished, while the tensioned membrane effect is enhanced.

(5) Using embankment surface settlement and the stress concentration ratio between piles and soil as key control indices, the elastic modulus, tensile stiffness, and friction angle of the GRSP are identified as the three most critical design parameters. Specifically, based on our case studies, we recommend using materials with higher elastic modulus and greater friction angles, such as well-compacted sand or gravel, as the soil platform. Additionally, incorporating high-strength

geogrids as reinforcement in the GRSP is advised to effectively reduce the overall settlement of the embankment. However, beyond these three parameters, the placement of geogrids within the GRSP has a negligible impact on the performance of the pile-supported embankment.

Data availability statement

The original contributions presented in the study are included in the article/Supplementary Material; further inquiries can be directed to the corresponding author.

Author contributions

ZZ: data curation, investigation, methodology, software, and writing–original draft. LZ: conceptualization, supervision, and writing–review and editing.

Funding

The author(s) declare that financial support was received for the research, authorship, and/or publication of this article. The authors acknowledge financial support from the National Science Foundation of China (No. 51890912).

Conflict of interest

Author ZZ was employed by Suzhou New District Testing Corporation.

The remaining author declares that the research was conducted in the absence of any commercial or financial relationships that could be construed as a potential conflict of interest.

The reviewer XN declared a shared affiliation with the author LZ to the handling editor at the time of review.

Publisher's note

All claims expressed in this article are solely those of the authors and do not necessarily represent those of their affiliated organizations, or those of the publisher, the editors, and the reviewers. Any product that may be evaluated in this article, or claim that may be made by its manufacturer, is not guaranteed or endorsed by the publisher.

References

Badakhshan, E., Noorzad, A., Bouazza, A., Zameni, S., and King, L. (2020). A 3D-DEM investigation of the mechanism of arching within geosynthetic-reinforced piled embankment. *Int. J. SOLIDS Struct.* 187, 58–74. doi:10.1016/j.ijsolstr.2019.03.035

Blanc, M., Rault, G., Thorel, L., and Almeida, M. (2013). Centrifuge investigation of load transfer mechanisms in a granular mattress above a rigid inclusions network. *Geotext. Geomembr.* 36, 92–105. doi:10.1016/j.geotexmem.2012.12.001

Borges, J. L., and Marques, D. O. (2011). Geosynthetic-reinforced and jet grout column-supported embankments on soft soils: numerical analysis and parametric study. *Comput. Geotech.* 38, 883–896. doi:10.1016/j.compgeo.2011.06.003

Briançon, L., and Simon, B. (2012). Performance of pile-supported embankment over soft soil: full-scale experiment. *J. Geotech. Geoenvironmental Eng.* 138, 551–561. doi:10.1061/(ASCE)GT.1943-5606.0000561

Chen, R. P., Xu, Z. Z., Chen, Y. M., Ling, D. S., and Zhu, B. (2010). Field tests on pile-supported embankments over soft ground. *J. Geotech. Geoenvironmental Eng.* 136, 777–785. doi:10.1061/(ASCE)GT.1943-5606.0000295

Du, W., Nie, R., Qi, Y., Ruan, B., and Mo, F. (2024). Investigation on the static performance of geogrid reinforced aeolian sand railway embankment: field test and discrete element simulation. *Geotext. Geomembr.* 52, 736–752. doi:10.1016/j.geotexmem.2024.03.012

Esmaeili, M., Naderi, B., Neyestanaki, H. K., and Khodaverdian, A. (2018). Investigating the effect of geogrid on stabilization of high railway embankments. *Soils Found.* 58, 319–332. doi:10.1016/j.sandf.2018.02.005

Ghosh, B., Fatahi, B., Khabbaz, H., Nguyen, H. H., and Kelly, R. (2021). Field study and numerical modelling for a road embankment built on soft soil improved with concrete injected columns and geosynthetics reinforced platform. *Geotext. Geomembr.* 49, 804–824. doi:10.1016/j.geotexmem.2020.12.010

Han, J., and Gabr, M. A. (2002). Numerical analysis of geosynthetic-reinforced and pile-supported earth platforms over soft soil. *J. Geotech. Geoenvironmental Eng.* 128, 44–53. doi:10.1061/(ASCE)1090-0241(2002)128:1(44)

Huang, J., and Han, J. (2010). Two-dimensional parametric study of geosynthetic-reinforced column-supported embankments by coupled hydraulic and mechanical modeling. *Comput. Geotech.* 37, 638–648. doi:10.1016/j.compgeo.2010.04.002

Huang, J., Han, J., and Oztoprak, S. (2009). Coupled mechanical and hydraulic modeling of geosynthetic-reinforced column-supported embankments. *J. Geotech. Geoenvironmental Eng.* 135, 1011–1021. doi:10.1061/(ASCE)GT.1943-5606.0000026

Khosrojerdi, M., Qiu, T., Xiao, M., and Nicks, J. (2018). Numerical investigation on the performance of geosynthetic-reinforced soil piers under axial loading: 3rd international foundation congress and equipment expo 2018: developments in earth retention, support systems, and tunneling, IFCEE 2018. *Geotech. Spec. Publ. 2018-March*, 99–108. doi:10.1061/9780784481608.010

Liu, H., Kong, G., Chu, J., and Ding, X. (2015). Grouted gravel column-supported highway embankment over soft clay: case study. *Can. Geotech. J.* 52, 1725–1733. doi:10.1139/cgj-2014-0284

Liu, H. L., Ng, C. W. W., and Fei, K. (2007). Performance of a geogrid-reinforced and pile-supported highway embankment over soft clay: case study. *J. Geotech. Geoenvironmental Eng.* 133, 1483–1493. doi:10.1061/(ASCE)1090-0241(2007)133:12(1483)

McNulty, J. (1965). An experimental study of arching in sand. Available at: https://api.semanticscholar.org/CorpusID:108153817.

Okyay, U. S., Dias, D., Thorel, L., and Rault, G. (2014). Centrifuge modeling of a pile-supported granular earth-platform. *J. Geotech. Geoenvironmental Eng.* 140, 04013015. doi:10.1061/(ASCE)GT.1943-5606.0001004

Pham, H. T. V., Suleiman, M. T., and White, D. J. (2004). Numerical analysis of geosynthetic-rammed aggregate pier supported embankments. *Geotech. Eng. Transp. Proj.*, 657–664. doi:10.1061/40744(154)52

Rowe, R. K., and Liu, K.-W. (2015). Three-dimensional finite element modelling of a full-scale geosynthetic-reinforced, pile-supported embankment. *Can. Geotech. J.* 52, 2041–2054. doi:10.1139/cgj-2014-0506

Rui, R., Han, J., van Eekelen, S. J. M., and Wan, Y. (2019). Experimental investigation of soil-arching development in unreinforced and geosynthetic-reinforced pile-supported embankments. *J. Geotech. Geoenvironmental Eng.* 145, 04018103. doi:10.1061/(ASCE)GT.1943-5606.0002000

Shen, P., Xu, C., and Han, J. (2020). Geosynthetic-reinforced pile-supported embankment: settlement in different pile conditions. *Geosynth. Int.* 27, 315–331. doi:10.1680/jgein.19.00015

Stewart, M. E., and Filz, G. M. (2005). "Influence of clay compressibility on geosynthetic loads in bridging layers for column-supported embankments," in *Contemporary issues in foundation engineering* (Austin, Texas, United States: American Society of Civil Engineers), 1–14. doi:10.1061/40777(156)8

Stewart, M. E., Navin, M. P., and Filz, G. M. (2004). Analysis of a column-supported test embankment at the I-95/Route 1 interchange. *Geotech. Eng. Transp. Proj.*, 1337–1346. doi:10.1061/40744(154)123

Terqueux, C., Racinais, J., Briançon, L., Pantet, A., and Gotteland, P. (2023). "Full scale experiment of a geosynthetic-reinforced piled embankment," in *Geosynthetics: leading the way to a resilient planet* (London: CRC Press).

Terzaghi, K. (1936). Stress distribution in dry and in saturated sand above a yielding trap-door. Available at: https://api.semanticscholar.org/CorpusID:132913229.

Terzaghi, K. (1943). *Theoretical soil mechanics*. John Wiley and Sons.

van Eekelen, S. J. M., Venmans, A. a. M., Bezuijen, A., and van Tol, A. F. (2020). Long term measurements in the Woerden geosynthetic-reinforced pile-supported embankment. *Geosynth. Int.* 27, 142–156. doi:10.1680/jgein.17.00022

Wu, D., Luo, C., Gao, Z., Li, D., and Xu, C. (2022). Effect of different reinforced load transfer platforms on geosynthetic-reinforced pile-supported embankment: centrifuge model test. *KSCE J. Civ. Eng.* 26, 630–649. doi:10.1007/s12205-021-0623-7

Xing, H., Zhang, Z., Liu, H., and Wei, H. (2014). Large-scale tests of pile-supported earth platform with and without geogrid. *Geotext. Geomembr.* 42, 586–598. doi:10.1016/j.geotexmem.2014.10.005

Xu, C., Wu, D., Song, S., and Liu, B. (2018). "Centrifuge model tests of basal reinforcement effects on geosynthetic-reinforced pile-supported embankment," in *Proceedings of geoshanghai 2018 international conference: ground improvement and geosynthetics*. Editors L. Li, B. Cetin, and X. Yang (Singapore: Springer-Verlag Singapore Pte Ltd), 279–287. doi:10.1007/978-981-13-0122-3_31

Yan, M., Song, X., Xiao, H., Guo, S., Zhang, H., and Chango, I. V. L. (2022). Analysis of load transfer in geosynthetic-reinforced pile-supported embankments. *2022 16TH IEEE Int. Conf. SIGNAL Process. (ICSP2022)* 1, 354–358. doi:10.1109/ICSP56322.2022.9965213

Zhang, X., Zhuang, Y., Hu, S., and Dong, X. (2022). A simplified method for assessing the serviceability performance of geosynthetic reinforced and pile-supported embankment. *Geotext. Geomembr.* 50, 1214–1229. doi:10.1016/j.geotexmem.2022.08.006

Zhou, M., Liu, H., Chen, Y., and Hu, Y. (2016). First application of cast-in-place concrete large-diameter pipe (PCC) pile-reinforced railway foundation: a field study. *Can. Geotech. J.* 53, 708–716. doi:10.1139/cgj-2014-0547